IEEE Access
Multidisciplinary | Rapid Review | Open Access Journal

Received 22 December 2022, accepted 10 January 2023, date of publication 16 January 2023, date of current version 25 January 2023.

Digital Object Identifier 10.1109/ACCESS.2023.3237326

RESEARCH ARTICLE

Smart Local Energy Systems: Optimal Planning of Stand-Alone Hybrid Green Power Systems for On-Line Charging of Electric Vehicles

HANI GHARAVI AHANGAR[1], (Member, IEEE), WENG KEAN YEW[2], (Member, IEEE), AND DAVID FLYNN[3], (Member, IEEE)

[1]Elgin Energy, Dublin 2, D02 WV96, Ireland
[2]School of Engineering and Physical Sciences, Heriot-Watt University Malaysia, Putrajaya 62200, Malaysia
[3]James Watt School of Engineering, University of Glasgow, G12 8QQ Glasgow, U.K.

Corresponding author: Weng Kean Yew (w.yew@hw.ac.uk)

This work was supported in part by the Engineering and Physical Sciences Research Council (EPSRC) funded by the U.K. National Centre for Energy Systems Integration (CESI) under Grant EP/P001173/1, and in part by the Innovate U.K. ReFLEX Project under Grant 104780.

ABSTRACT Multi-vector smart local energy systems are playing an increasingly importantly role in the fast-track decarbonisation of our global energy services. An emergent contributor to global decarbonisation is green hydrogen. Green hydrogen can remove or reduce the burden of electrification of heat and transport on energy networks and provide a sustainable energy resource. In this paper, we explore how to optimally design a standalone hybrid green power system (HGPS) to supply a specific load demand with on-line charging of Electric Vehicles (EV). The HGPS includes wind turbine (WT) units, photovoltaic (PV) arrays, electrolyser and fuel cell (FC). For reliability analysis, it is assumed that WT, PV, DC/AC converter, and EV charger can also be sources of potential failure. Our methodology utilises a particle swarm optimization, coupled with a range of energy scenarios as to fully evaluate the varying interdependences and importance of economic and reliability indices, for the standalone HGPS. Our analysis indicates that EV charging with peak loading can have significant impact on the HGPS, resulting in significant reductions in the reliability indices of the HGPS, therefore enhance the operation of HGPS and reduces the overall cost. Our analysis demonstrates the importance of understanding local demand within a multi-vector optimization framework, as to ensure viable and resilient energy services.

INDEX TERMS Smart local energy system, green hydrogen, reliability, economics, optimization, electric vehicle charging.

NOMENCLATURE

ACRONYMS

BES	Battery Energy Storage.
DGs	Distributed Generation Sources.
EENS	Expectation Of Not Served Energy.
ELF	Equivalent Loss Factor.
ESS	Energy Storage System.
EV	Electric Vehicle.
FC	Fuel Cell.
GA	Genetic Algorithm.
HGPS	Hybrid Green Power System.
HST	Hydrogen Storage Tank.
LOE	Loss of Energy.
LOEE	Loss Of Energy Expectation.
LOLE	Loss Of Load Expectation.
LPSP	Loss Of Power Supply Probability.
PSO	Particle Swarm Optimization.
PV	Solar Photovoltaic.
RES	Renewable Energy Sources.
SLES	Smart Local Energy Systems.
V2G	Vehicle-to-grid.

The associate editor coordinating the review of this manuscript and approving it for publication was Frederico Guimarães.

V2H Vehicle-to-home.
V2V Vehicle-to-vehicle.
WT Wind Turbine.

VARIABLES AND PARAMETERS

A Coefficient for wind speed.
A_{inv} Probability of being available for inverter.
A_{PV} Probability of being available for PVarray.
A_{WT} Probability of being available for WT.
A_{chr} Probability of being available for EV charger.
$\mathrm{BZ}_{\mathrm{brand}}$ Battery size of each brand.
C Cost function.
$\mathrm{Chr}_{\mathrm{req}}$ Charging required for each EV.
C_{loss} Average cost of loss due to unmet load (\$/kWh).
C_{max} Maximum value of cost function.
$\mathrm{C}_{\mathrm{min}}$ Minimum value of cost function.
CC_i Initial investment cost equipment i (\$/unit).
C_{total} Total cost of HGPS (\$).
D Vector described by P-R.
D (t) Load demand for tth (kW).
$E_{HST}(t)$ Energy stored in the HST at time step t (kW).
ELF_{max} Maximum equivalent load failure.
$E[X]$ Mathematical expectation.
f Inflation rate.
f_{HGPS} Probability function for PV and WT.
f_{system} Probability function for PV and WT and inverter.
$G_H(t)$ Horizontal element of solar irradiation (W/m^2).
$G_V(t)$ Vertical element of solar irradiation (W/m^2).
$G(t, \theta_{PV})$ Incident solar irradiation perpendicular to panel surface at time step t and Installation angle (W/m^2).
h WT-Height (m).
h_{ref} Reference height (m).
HHV_{H_2} Higher heating value of hydrogen (39.7 kWh/kg).
i Index of equipment.
$\mathrm{In}_{\mathrm{chr}}$ Initial charge of each EVs.
ir Real interest rate.
ir_{nom} Nominal interest rate.
K Factor to convert replacement cost into a single present cost.
L Useful lifetime.
$LOE(t)$ Loss of energy for tth.
$LOL(t)$ Loss of load for tth.
m Counter.
$m_{HST}(t)$ Mass of hydrogen in HST in time step t (kg).
M_{HST} Capacity of HST (kW).
MC_i O&M cost of equipment i (\$/kWh).
$mean$ Function for meaning.
n Counter.
N Number of times that load is lost.
N_i Number of installed equipment i (kW or kg).
N_{PV} Total number of PV.
N_{var} Number of dimensions of problem.
N_{WT} Total number of WT.
n_{PV}^{fail} Number of failures of PV.
n_{WT}^{fail} Number of WT failures.
NPC_i Net present cost of equipment i (\$/kWh).
NPC_{loss} Net present cost of unmet load (\$/kWh).
$Penalty$ Penalize the objective function where the reliability indices are violated (for each time violation, Penalty gets bigger with adding to a coefficient 1010(\$)).
$P_{el-HST}(t)$ Output power of electrolyser at time step t (kW).
$P_{FC-inv}(t)$ FC output power delivered to inverter (kW).
$P_{furl}(t)$ Output power of WT at cut-out wind speed (kW).
$P_{HGPS-el}(t)$ Input power to electrolyser at time step t (kW).
$P_{HGPS-inv}(t)$ Injected power to inverter from renewable resources at time step t (kW).
$P_{HGPS}\left(n_{WT}^{fail}, n_{PV}^{fail}\right)$ Purchased power by HGPS components with failure probability.
$P_{HGPS}(t)$ Generated power by HGPS in time step t (kW).
$P_{HST-FC}(t)$ Power of the HST injected to FC at time step t (kW).
$P_{inv-load}(t)$ Injected power to the load at time step t (kW).
$P_{load}(t)$ Load demand in time step t (kW).
P_{PV} Output power of PV array (kW).
$P_{PV,rated}$ Rated power of each PV array at $G = 1000$W/m2.
Pr_{int} Percentage initial charge of each EV.
P_s Probability of state s occurrence.
P_{WT} WT output power (kW).
$P_{WT,max}$ Maximum output power of WT (kW).

PWA	Factor to convert operational cost into a single present cost.
Q_s	Lost load at state s occurrence (kWh).
R	Vector with the same dimension as P.
r	Random number with uniform distribution.
RC_i	Replacement cost of equipment i ($/unit).
$round$	Function for rounding.
S	Set of all possible states.
t	Time step index.
T_s	Duration of loss of load at state s.
$v_{cut\ in}$	Cut-in wind speed of WT (m/s).
$v_{cut\ out}$	Cut-out wind speed of WT (m/s).
v_{rated}	Rated wind speed (m/s).
v_W	Wind speed (m/s).
v_W^h	Wind speed at a given installation height h (m/s).
v_W^{ref}	Wind speed at reference height (m/s).
z	Constant.
η_{el}	Electrolyser efficiency.
η_{FC}	FC efficiency.
η_{HST}	Efficiency of HST.
η_{inv}	Inverter efficiency.
$\eta_{PV,conv}$	The efficiency of PV's DC/DC converter and Maximum Power Point Tracking System (MPPT).
Δt	Simulation Time step (1 hour).
ψ	Constant (0.14-0.25).
θ	Add a value working as an angle to x.
θ_{PV}	Installation angle of PV array (deg).

I. INTRODUCTION

In the global response to the climate change crisis, access to affordable renewable energy resources (RES) represents a key element of both a global environmental response, but is also a primary requirement of an inclusive energy transition [1]. The needs of communities and the associated infrastructure throughout the world is highly variable, understanding this local energy demand is vital to future solutions [2], [3]. Improving the utilisation of locally generated renewable energy is vital not only to the decarbonisation of primary energy services e.g., heating, cooling, light etc., but local energy systems must also support the new energy demand of decarbonised transport which is becoming increasingly coupled to these local energy services. This has created a catalyst for exponential growth in the deployment of RES and also presents new challenges to energy networks, both on grid and hybrid, in terms of managing new uncertainties in energy demand profiles coupled with network constraints e.g. voltage violations [4]. Therefore, the optimization of energy systems and services, represents a complex social, techno-economic and environmental challenge [5], [6], [7]. With an emphasis on the challenges of communities in remote locations or with limited/constrained energy infrastructure, hybrid green power systems (HGPSs), which commonly incorporate renewable energy sources (RESs) such as wind turbine (WT) and solar photovoltaics (PV), have made significant progress in electricity production over the past decade [8]. Such hybrid energy solutions, albeit not necessarily coupled to an existing energy network, still represent a complex multi-objective optimization if they are to deliver resilient, reliable and affordable energy services [9]. With the integration of RESs into the HGPS, significant reductions can be made in terms of carbon dioxide emission from fossil fuel consumption. However, intermittent output power from RESs needs to be addressed as part of their integration into the HGPS [10]. This is a key concern since RES are unreliable as standalone technologies due to the mechanism of generation not necessarily being coupled to energy demand requirements.

To overcome this variability in supply, the fluctuating power from the RES must be integrated with other complementary distributed generation sources (DGs) such as energy storage systems (ESS) to improve the system's reliability. Commonly, for HGPS, battery energy storage (BES) is used as the ESS to store the excess generation from the RES [11], [12], [13]. Subsequently, BES is discharged when the RES is less than the demand to ensure continuous power supply to the varying load. Alternatively, a Fuel Cell (FC) was used as the ESS by authors in [14] and [15] for stand-alone HGPS. For this HGPS, the excess generation from the RES is used to power the electrolyser to produce hydrogen which is stored in the hydrogen storage tanks. The FC can then be used as a backup source of power when the RES is not available or sufficient to meet the load demand. Authors in [15] also compared the economic analysis on various combinations of stand-alone HGPS alongside ESS such as BES and FC for a commercial centre load supply. This analysis suggests that stand-alone HGPS should consists of both PV and WT alongside the ESS to improve system reliability and reduce the overall costs of the system. However, HGPS with ESS will result in significantly higher capital expenditure as the ESS are typically oversized to improve reliability of the HGPS. Thus, there is a need to identify the optimal combination for the DGs within a HGPS using sizing optimization.

Many optimization techniques have been documented in literature to identify the optimal size of HGPS based on reliability and cost. Loss of power supply probability (LPSP) is commonly used as a reliability index in sizing of HGPS optimization because it can calculate how frequent a system is able to sustain a loss of power supply within a period of time [16], [17]. Authors in [17], [18], [19], and [20] utilized LPSP as the reliability index while seeking to minimize the annualized cost of the system. Optimization was done using genetic algorithm (GA) [21], [22] and fuzzy logic [23] to determine the optimal configuration for a stand-alone HGPS. Simulated annealing optimization strategy was also used in [24] to size the stand-alone HGPS, where the objective

function was to minimize the total energy costs. By using the wind speed, solar irradiation and load demand data, an optimization was done in [25], [26], and [27] using particle swarm optimization (PSO) to obtain the optimal units for the standalone HGPS. Application of various optimization methods to obtain the optimal size of HGPS can be found in literature. However, the application of optimization of HGPS for online charging of electric vehicles is found to be less in the literature.

Electric vehicles (EV) are seen as a promising technology to tackle the climate change issue and a replacement to the traditional road transportation technology that are dependent on the depleting fossil fuel supply [28]. This is because the source of energy of an EV comes solely from the battery on board [29]. However, EVs require frequent charging as its driving range is much shorter compared to traditional transportation [30]. Hence, efforts are focused on installing charging infrastructure as to accommodate the growth of EV worldwide [31]. Although EVs have many green benefits, it is seen as a load from the distribution network perspective [32]. If there is a large growth of EVs in a distribution network, it will lead to an increased load demand when the EV requires charging. If the charging is conducted simultaneously, it can affect the overall grid stability and the power quality as well. Apart from that, grid operators may also be facing with other power issues such as unfavourable peaks in demand or reduced reserve margin [33]. Hence, solutions to mitigate the impact of EV charging on the distribution network are being developed by researchers.

Authors in [34] proposed a load management scheme by scheduling and coordinating the EV charging to minimize the peak loads and improve grid stability. Similarly, EV charging load scheduling was also implemented in [32] and [35] to match the excess energy from the RES as an additional form of ESS. Apart from that, advance concepts such as Vehicle-to-Grid (V2G), Vehicle-to-Vehicle (V2V) and Vehicle-to-Home (V2H) are also being developed to allow EV to sell electricity by discharging the EV battery [36]. In the ideal situation, the EV would then be able to support the grid as a reserve generation or load, similar to an ESS, to further improve the grid stability.

There is already extensive literature that explores the varying levels of complex techno-economic analysis of DG and storage technologies. Given the importance of distributed multi-vector SLES, in terms of their requirement to meet key performance criteria e.g. reliability, decarbonisation and affordability, and whilst being inclusive of a range of multi-vector technologies our research focuses on HPGS-FC. Such multi-vector energy systems and hydrogen technologies are typically relevant to constrained network scenarios with curtailed green (renewable energy) [37], [38]. For example, Hydrogen is a valid decarbonised energy vector for the service needs of transport such as HGVs [39] and heating solutions [40]. Considering future trends there are also potential risks associated with the cost, availability and sustainability

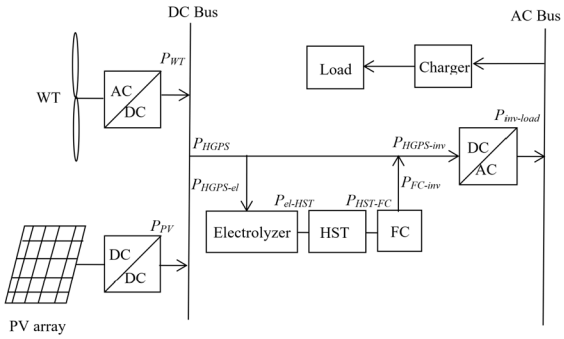

FIGURE 1. HGPS structure used in this study.

of other storage solutions such as Li-ion batteries, due to limited global reserves of lithium, cobalt, rare earth elements, lifecycle, ethical sustainability, etc ([41], [42]). Hence, our research focuses on creating a transferable methodology to address open research questions associated with the future sustainability of SLES while providing a valuable contribution to both optimised of SLES and the context of hydrogen technology inclusion.

On examination of the literature, the contributions of the paper are as follows:

- EV load patterns using a multi-vector standalone HGPS has not addressed the interdependent reliability and economic requirements of an operating energy system solution. Hence, the objective of this study is to optimally design a multi-vector standalone HGPS to supply a fleet of EVs during a full year with considerations for economic and reliability indices.
- The HGPS includes WT units, PV array, electrolyser, and FC to represent a multi-vector energy system and actual data used for simulation are annual solar irradiation and wind speed for the northwest region of Iran.
- EV demands were modelled based on various car brands and with random initial state of charge and random plug-in and out duration for different days of a week including weekends to better represent a realistic case.
- For optimization, due to the discontinuity of variables and non-linearity of the objective function, Particle Swarm Optimization (PSO) is selected for this study.

The remainder of our paper is structured as follows; Section II will describe the problem formulation including HGPS and reliability modelling. Then, the objective problem solving for the applied PSO are outlined in Section III followed by the simulation result and discussions in section IV.

II. FRAMEWORK

'For the standalone HGPS, the system operates independent from the electrical network. As shown in Figure 1, the HGPS feeds the load via EV chargers and consists of WT units, PV array, electrolyser, Hydrogen Storage Tank (HST), FC units, and DC/AC inverter. All variables and symbols are explained in the nomenclature section.

The total produced power by the HGPS is the sum of WT and PV outputs. In each hourly time step, one of the following conditions exists:

(a) All generated power by HGPS, P_{HGPS} is sent to DC/AC bus to supply load demand through EV chargers,

$$P_{HGPS}(t) = \frac{P_{load}(t)}{\eta_{inv} \times \eta_{chr}} \tag{1}$$

(b) Excess power is delivered to electrolyser to produce hydrogen, then whenever transferred power to electrolyser is more than its rated capacity or HST reaches its maximum capacity, excess power is dissipated by means of a dump load,

$$P_{HGPS}(t) > \frac{P_{load}(t)}{\eta_{inv} \times \eta_{chr}} \tag{2}$$

(c) Portion of load demand not supplied by WT and PV is met by FC and electrical network,

$$P_{HGPS}(t) < \frac{P_{load}(t)}{\eta_{inv} \times \eta_{chr}} \tag{3}$$

Note that whenever the sum of FC is not adequate to supply load demand, there is an increase in loss of reliability, as discussed and analyzed in details later.

A. MODELLING OF HGPS COMPONENTS

1) WIND TURBINE

The power output, P_{WT} in regard to wind speed, v_w can be calculated as:

$$P_{WT} = \begin{cases} 0; & v_W \le v_{cuti}, v_W \ge v_{cutout} \\ P_{WT,\max} \times \left(\dfrac{v_W - v_{cutin}}{v_{rated} - v_{cutin}} \right)^z; & v_{cutin} \le v_W \le v_{nuted} \\ P_{WT,\max} + \dfrac{P_{fwrl} - P_{WT,\max}}{v_{cutout} - v_{ruted}} \times (v_W - v_{ruted}); & v_{ruted} \le v_W \le v_{cutout} \end{cases} \tag{4}$$

In our study, v_{cutin}, v_{cutout} and v_{rated} are 3, 25, and 13 m/s, respectively. In addition, P_{furl} and $P_{WT,max}$ are considered 5.8 and 8.1 kW, respectively. Parameter z is a constant (assumed = 3) [10].

Wind speed at a given installation height is modelled by the exponent law [10].

$$v_W^h = v_W^{ref} \times \left(\frac{h}{h_{ref}} \right)^{\psi} \tag{5}$$

where ψ is the exponent law coefficient which varies between 0.14 and 0.25 depending on the landscape. For this study, a value of 0.14 is used which represents a relatively flat surface.

TABLE 1. Costs and specifications of HGPS equipment [44], [45], [46].

Equipment	CC ($/unit)	RC ($/unit)	MC ($/unit-year)	L (year)	η (%)	unit	Availability (%)
WT	3,200	2,700	75	20	-	7.5 (kW)	96
PV array	2,000	1,700	20	20	-	1 (kW)	96
Electrolyzer	2,000	1,500	25	20	75	1 (kW)	100
HST	1,300	1,200	15	20	95	1 (kg)	100
FC	4,000	3,500	300	5	50	1 (kW)	100
Inverter (DC/AC)	800	750	8	15	90	1 (kW)	99.89
EV charger	3000	3000	0	10	96	19.2 (kW)	90

2) PV ARRAY

The power from PV array is modelled as [27]

$$P_{PV} = \frac{G(t, \theta_{PV})}{1000} \times P_{PV,rated} \times \eta_{PV,conv} \tag{6}$$

$$G(t, \theta_{PV}) = G_V(t) \times \cos(\theta_{PV}) + G_H(t) \times \sin(\theta_{PV}) \tag{7}$$

PV systems are typically connected to a MPPT, either together with their DC-DC converters or inverters, in order to maximize the output power. Thus, in our study, we have connected the PV arrays with a MPPT with an efficiency of 95% ($\eta_{PV,conv} = 95\%$). It is important to note that the effects caused by temperature are not considered in this study.

3) HYDROGEN STORAGE TANK

The energy stored in the HST at each hourly time step (Δt) is [27]

$$E_{HST}(t) = E_{HST}(t-1) + P_{el-HST}(t) \times \Delta t - P_{HST-FC}(t) \times \Delta t \times \eta_{HST} \tag{8}$$

From there, the mass of hydrogen in the HST, m_{HST} can be calculated and is given as [43]

$$m_{HST}(t) = \frac{E_{HST}(t)}{HHV_{H_2}} \tag{9}$$

where HHV_{H_2} is the Higher Heating Value of hydrogen and is equal of 39.7kWh/kg [43]. Note that in order to store produced power by electrolyser in the hydrogen tank in form of hydrogen, a compression of hydrogen is required which results to energy loss. This value is captured in η_{HST}.

4) ELECTROLYSER

The relation between output and input power of electrolyser is [27]

$$P_{el-HST}(t) = P_{HGPS-el}(t) \times \eta_{el} \tag{10}$$

It is important to note here that the electrolyser efficiency, η_{el} is assumed as constant for all operating conditions.

5) FUEL CELL

The FC output power delivered to inverter, P_{FC-inv} is [27]

$$P_{FC-imv}(t) = P_{HST-FC}(t) \times \eta_{FC} \tag{11}$$

The FC efficiency, η_{FC} is assumed as constant for all operating conditions as well.

6) INVERTER

The effect of inverter is modelled by its efficiency as [27]

$$P_{inv-load}(t) = (P_{FC-inv}(t) + P_{HGPS-inv}(t)) \times \eta_{inv} \quad (12)$$

7) EV CHARGER

The effect of EV charger is modelled by its efficiency as

$$P_{chr-load}(t) = P_{inv-chr}(t) \times \eta_{chr} \quad (13)$$

B. OBJECTIVE FUNCTIONS

In this study, to address various approaches that may be used for design analysis of HGPS, four types of objective functions are formulated as one objective function using weighting factor technique with equal weighting to treat all objectives similarly [48]. The expected useful life of equipment is based on Table 2 and all terms in the objective functions are converted to the net present cost.

The first objective function considers the cost for capital investment and operation of the HGPS, given by

$$Min\{C_{total}\} = \sum_i NPC_i + NPC_{loss} + Penalty \quad (14)$$

For the HGPS examined, Eq. (14) is formulated to find the optimum number of WT units and panels in PV array, installation angle of PV array, and capacity of electrolyser, FC, DC/AC inverter, HST and number of EV charger units. In general, the operational costs and capital investments of equipment used is

$$NPC_i = N_i\,(CC_i + RC_iK + MC_iPWA) \quad (15)$$

where K and PWA are factors to convert replacement and operational costs into a single present cost, respectively, defined as

$$K = \sum_{n=1}^{Y} \frac{1}{(1+ir)^{L\times n}} \quad (16)$$

and

$$PWA = \frac{(1+ir)^n - 1)}{ir(1+ir)^n} \quad (17)$$

where

$$ir = \frac{(ir_{nom} - f)}{(1+f)} \quad (18)$$

The costs of loss of energy expectation ($LOEE$) or expected energy not supplied represents the penalty that must be paid for energy not supplied to meet load demand by HGPS and it appears in the term that accounts for losses,

$$NPC_{loss} = LOEE \times C_{loss} \times PWA \quad (19)$$

And the third term of Eq. (14) ($Penalty$), a large number greater than 10^{15} depending the total cost, is considered to penalize the objective function where the reliability indices are violated.

The second objective function considers the cost for capital investment and operation of the HGPS located at a distance from the site, as follows

$$Min\{C_{total}\} = \sum_i NPC_i + NPC_{loss} + Penalty \quad (20)$$

In Eq. (20), the first term accounts for operational costs and capital investments of equipment for HGPS, where the operational cost is equal to maintenance cost with no consideration for fuel cost. The second term is described by Eq. (18). The third term is the penalty for violation of the reliability indices. Note that the significance of penalty terms in Eqs. (14) and (20) are discussed later, when reliability indices are introduced.

The optimal design problem of HGPS is accomplished in three different scenarios, where the above-described objective functions are utilized on individual basis or in combination. For totally reliable HGPS (Case 1) with a very high cost for LOE, there is no concern with regard to reliability indices and the optimal design problem is solved in a single-objective form based on Eq. (14) taking into account the fact that the cost of LOE is high enough so that the optimal design is in a way to avoid any load loss. For the second scenario, reliability indices are considered and cost of LOE is not severely penalized so that the optimal design of HGPS would be chosen in a way to consider all these elements. For the third scenario, the optimal design system is examined on two daily load profiles that are not similar to the original yearly load profile and are produced again using the algorithm explained in details for the load profile production later in this study. The idea is to see if the optimal design system is good enough to provide a newly generated load with minimum load loss considering all the reliability indices.

C. RELIABILITY INDICES

The probability is that a device functions properly to participate in supplying the load demand, under operating condition during a specific period of time, is discussed in [10]. The various indices defined in the literature for calculating reliability level include loss of load expectation ($LOLE$), $LOEE$, loss of power supply probability ($LPSP$), and equivalent loss factor (ELF) given in [1] and [18]:

$$LOLE = \sum_{t=1}^{N} E\,[LOL\,(t)] \quad (21)$$

where

$$E\,[LOL] = \sum_{s\in S} T_s \times P_s \quad (22)$$

$$LOEE = \sum_{t=1}^{N} E\,[LOE\,(t)] \quad (23)$$

where

$$E\,[LOE(t)] = \sum_{s\in S} Q_s \times P_s \quad (24)$$

$$LPSP = \frac{LOEE}{\sum_{t=1}^{N} D(t)} \tag{25}$$

$$ELF = \frac{1}{N} \sum_{t=1}^{N} \frac{Q(t)}{D(t)} \tag{26}$$

It must be noted that ELF incorporates more information about both the number of outages and the amount of not supplied load demand [27]. In this study, all above 4 formulates indices represented by Eqs. (21), (23), (25), and (26) are calculated and presented in terms of an average value for the year (8760 h). The maximum permissible ELF in the developed countries is considered as 0.0001 [27], however, for the standalone HGPS designed in this study, ELF is restricted to 0.01. Note that probability of encountering each state is calculated through binomial distribution function [27].

The assessment of reliability is carried out based on the assumption that failure is possible for WT units, PV array, DC/AC inverter, and EV charger while other equipment, such as, HST, electrolyser and FC are assumed 100% reliable. In this study, an approximate model for calculating the reliability is utilized. In the approximate model, the average produced power by WT units and PV array is exploited instead of considering single conditions for outage of WT units and PV array and, finally, the mathematical expectation of reliability indices is calculated. It is suggested to consider the output power of HGPS as its mathematical expectation [27]

$$E[P_{HGPS}] = N_{WT} \times P_{WT} \times A_{WT} + N_{PV} \times P_{PV} \times A_{PV} \tag{27}$$

where, P_{WT} and P_{PV} are the output power of wind turbines and photovoltaic arrays, respectively.

III. CONSTRAINTS

The objective function described by Eq. (14) is optimized subject to following constraints:

- *ELF* should not exceed an allowable value [27]

$$E[ELF] \leq ELF_{\max} \tag{28}$$

- Number of installed equipment is not negative

$$0 \leq N_i \tag{29}$$

- Installation angle of PV array is limited

$$0 \leq \theta_{PV} \leq {}^{\pi}/_{2} \tag{30}$$

- Energy stored in the HST at the end of year is not less than its value at the beginning.

$$E_{HST}(0) \leq E_{HST}(8760) \tag{31}$$

To guarantee meeting the reliability indices for the HGPS, the penalty terms in objective function given by Eq. (14) is assigned large values (in the order of 10^{15}) compared to the expected objective function value. When the reliability indices are met, the values for penalty terms are set to zero. Note that if the penalty terms are not added to the noted object, it is possible to arrive at solutions that correspond to lower costs without satisfying reliability indices.

IV. METHODOLOGY

A. OPTIMIZATION METHOD

Particle swarm optimization (PSO) is selected as the optimization method for our study due to the large number of variables and their discontinuity. PSO is a population-based metaheuristic optimization algorithm, inspired by the social behavior of birds and fish in nature, that have the capability to solve complex mathematical problems existing in engineering.

In PSO algorithm, firstly it is initialized with a population of random particles to identify the potential solutions, the variables set out in Table 4 with respect to the objective function given by equation (14). For every iteration these particles, which contain information of the variables and objective function, will then find their "best" positions (minimum objective function) and update the group based on the minimum values for the objective function and their associated variables per particle. If this is the group's "best", its' value is updated as well. After its evaluation, it will store the best values and will repeat the entire process again in search for the optimal solution until the maximum number of iterations is met. Figure 2 represents a flowchart for the PSO algorithm.

B. LOAD SETUP

In this study, we want to plan and test a hybrid renewable system that can feed a number of EV loads during a sample year. In order to size and plan the hybrid system, we need to know the load per hour over the year. In this regard, we need to create a meaningful demand that represents the EVs.

C. ASSUMPTIONS

We consider a leisure site that its charging station is only open from 16 to 4 every day. We assume that EVs are among the following brands with their corresponding battery sizes as shown in Table 2 [33]:

In addition, we assume that all the EVs that arrive to the site have an initial charging of a number between 20% - 80% of their battery sizes. The maximum charging power for the charger is 19.2 kW per hour given in Table 2. Note that the EV car brand and its initial charge is assigned to each car completely random for each day of the sample year. We also assume that a different number of EVs arrive at the site for different days of a sample week. The numbers of EVs that arrive on each day of the week are assumed as shown in Table 4. Note that seasonal effect was not considered in our EV demand modelling and it is assumed that EV demand varies per different day of a week including weekends for the full year. Therefore, we will have a varying load profile per different day of the year as shown in Figure 3.

Therefore, initial charge (energy storage) of each EV is calculated from the following equation:

$$\mathrm{In}_{\mathrm{chr}} = \mathrm{BZ}_{\mathrm{brand}} \times \mathrm{Pr}_{\mathrm{int}} \tag{32}$$

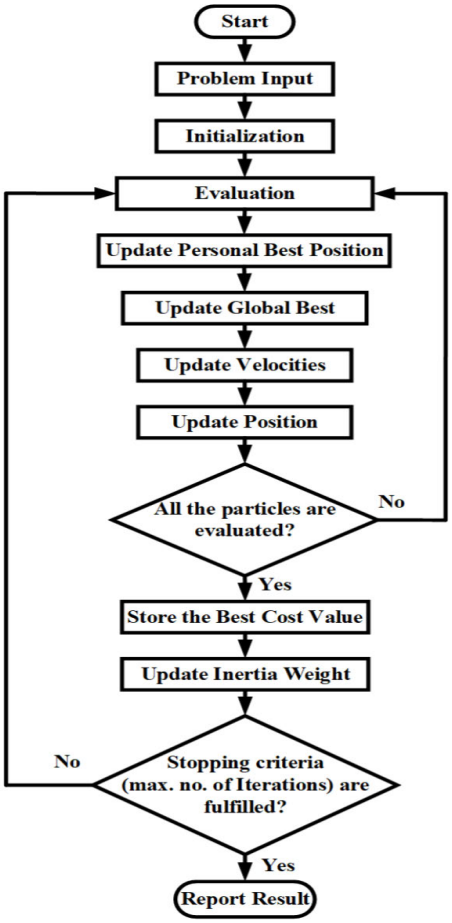

FIGURE 2. PSO algorithm flow chart [32].

where, In_{chr}, BZ_{brand} and Pr_{int} are initial charge of each EVs, battery size of each brand and percentage initial charge of each EVs, respectively. Thus, the kWh required to charge each EVs is calculated from the following equation:

$$Chr_{req} = BZZ_{brand} - In_{chr} \tag{33}$$

where, Chr_{req} is the charging required for each EVs.

The distribution of hourly number of EV arrivals to the site is assumed to follow a random number from beta distribution for a daily range from 16 to 23 of each day. Note that the pattern of EV arrivals differs daily based on the distribution for the year.

We assume that each EV stays at the site for either 2 or 5 hours and it assumed that 40% of cars stays at the site for 2 hours and the rest for 5 hours. This poses a constraint on the Chr_{req} for each EVs despite how much kWh charge is required for a particular EV. If the required charge takes longer than the time that the EV is staying at the site, then the EV is charged up to the point that it is staying at the charging station. The opposite term is also applicable when the required charge is less than the amount that can be delivered to the EV considering its time of staying at the site and the hourly kWh delivered to the EV by the charger. It is assumed that each EV is unplugged if it is fully charged despite its duration of staying at the site.

TABLE 2. EV brand and their corresponding battery size.

EVs		Battery Size (kWh)
Brand	Model	
Audi	e-tron	95
BMW	i3	42.2
Chevrolet	Bolt EV	65
Ford	Mustang SR	75.7
Ford	Mustang ER	98.8
Hyundai	IONIQ	38.3
Jaguar	IPACE	90
Porsche	Taycan	93.4
Tesla	Model S	100
Volkswagen	Pro S	82

TABLE 3. Number of EV arrive on each day of the week.

Week day	Number of cars arrive on each day
Saturday	50
Sunday	50
Monday to Thursday	10
Friday	30

D. RESULTANT LOAD

In order to moderate the randomness of the resultant load, we produced an average load profile from 100 various yearly load profiles for this study. The EV yearly demand is shown in Figure 3. Note that no V2G capability has been considered for this study.

V. RESULTS

The result section is divided to two sets of results. The first set of results express the first two scenarios of the paper related to reliability. We optimised HGPS components for two different scenarios: first when all the reliability indices are in place and we have a reasonable value for LOE cost. In the second scenario, we assumed that all the components are 100% available and the LOE cost is very high so that no load will be lost.

For the second set of results, we tested our optimised HGPS for two randomly generated daily loads for winter and summer for weekend and weekday, respectively.

A. HGPS OPTIMIZATION

In order to produce the results, it was required to have wind and solar radiation data as one of the inputs of the study. For this study, wind speed at the height of 15m and solar radiations data in the Northwest region of Iran were used as the inputs.

Figure 4 illustrates the convergence of PSO towards the optimum point for this problem from iteration 1 to 500 for two different scenarios 4(a) when the system is fully reliable

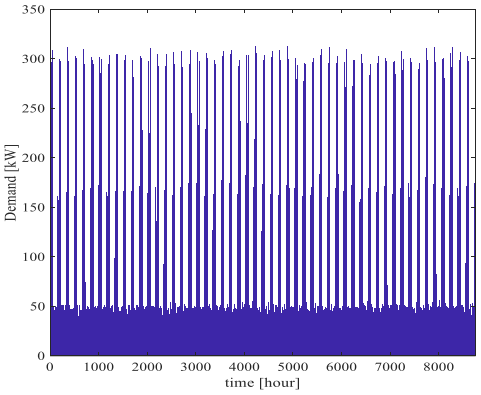

FIGURE 3. Yearly demand.

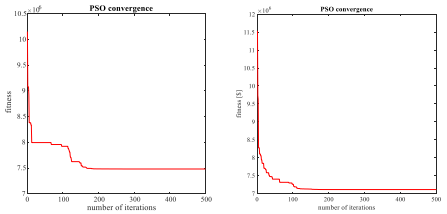

(a) (b)

FIGURE 4. PSO convergence for (a) full availability and (b) not 100% reliable.

and LOE cost is very high so that no load is allowed to be lost and 4(b) when the units reliabilities are considered and LOE cost is 5.6 US$/kWh. Number of particles in PSO for this study was 300. The planning horizon for this study is 20 years and the variables that need to be known for each individual scenario are shown in Table 4 for two different cases. Note that the outcome of PSO convergence depends on several factors such as swarm size, 200 in this study, number of iterations, 500 in this study, and acceleration coefficients together with the random vectors, control the stochastic influence of the cognitive and social components on the overall velocity of a particle. In this study, the optimization focuses on exploration in the early stages of optimization, while encouraging convergence to a good optimum near the end of the optimization process by attracting particles more towards the neighbourhood best (or global best) positions [49]. Experiments were run on a computer with 11th Gen Intel(R) Core (TM) i5-1145G7 @ 2.60GHz processor using 8 MB of RAM, running Windows version 11.

Table 4 shows optimal combinations of components in HGPS in this study for our scenarios. N_{WG}, N_{PV} and N_{chr} are 'number of WT, PV and EV charger units, respectively. P_{el}(kW), M_{tank}(kg), P_{FC}(kW) and P_{inv}(kW) show optimal capacity for electrolyser, storage tank, fuel cell and DC/AC inverter, respectively. θ_{PV}(degree) is also PV panels tilt angle in degrees. When all the units are 100% reliable and LOE cost is very high, then the system configurations will be in such a way to support the full load at any time given. The peak demand is 312.8 kW, which P_{inv}(kW), the size of inverter, and N_{chr}, the number of chargers, will be able to support considering their efficiencies. The maximum delivered power to chargers via inverter at peak load is P_{inv}(kW) $\times$ N_{chr} = 347.6 $\times$ 0.9 = 312.8 kW which is equal to the maximum demand.

N_{chr} is chosen to be 18 for the second scenario in this study which does not fully cover the peak demand (312.8 kW), 18 $\times$ 19.2 (kW) $\times$ η_{chr} (0.96) $\times$ A_{chr} (0.9)= 298.62 kW. η_{chr} is the efficiency of each EV charger unit. Therefore, we will have LOE during peak demand which will be penalized by LOE cost. It should be noted that the rated power of each WT unit is 7.5 kW, thus the optimal capacity of installed WT for the second scenario is N_{WG} (6) $\times$ $P_{rated,WG}$ (7.5 kW) = 45 kW. This capacity is significantly lower than the capacity of installed PV due to high cost associated with each WT unit.

Table 6 provides optimal costs including total cost, J (MUS$/yr), Investment cost (MUS$) and cost for loss of energy, AC_{loss} (MUS$/yr), and reliability indices including ELF, LOEE (MWh/yr), LPSP and LOLE (h/yr). As defined before, ELF should be lower than 0.01 in this study. There is almost 307 hours per year that the optimal solution cannot support EV drivers and 5.6 $/kWh penalty is considered for this. The corresponding lost energy due to LOLE value is 8.6 MWh/year for LOEE value and the penalty associated with LOEE is 0.6 MUS$/year, AC_{loss}.

Fig. 5 shows reliability indices (LOLE, LOEE and ELF) for a year in this study. As it can be seen from the graphs, the timing of the occurrences for all the indices is the same over the year.

B. ENERGY SCENARIOS

In order to assess how the optimal HGPS behaves in facing of a random daily load profile, two different energy scenarios are considered: In the first energy scenario, load is generated based on the strategy given in section V for week 5 of the year from 1st of January and on Saturday. The second energy scenario demand is generated for week 28 and for Tuesday.

Therefore, the first scenario is for winter and a busy day and the second scenario is for summer and a lightly loaded day (middle week). All the reliability factors are considered. This is true that the inverter is nearly impossible to fail for a sample day but we wanted to take its reliability factor into account which otherwise all the reliability indices would have been within in their ranges for any sample day that was not desirable.

Figure 6 shows the demands on 6(a) day 1 and 6(b) day 2. The demand on day 2 is significantly lighter the demand on day 1, nearly six times larger. The charging happens between 4 pm until 4 am next day.

Figure 7 illustrates the RES units output for the sample days 7(a) day 1 and 7(b) day 2. As can be seen, despite having a little bit difference in their magnitude and timing, the generations are quite similar for PV and WT units.

Figure 8 presents hourly expected amount of stored energy in the hydrogen tank during the sample 8(a) day 1 and 8(b) day 2. As can be seen the stored energy had risen in the tank when we had generations and then was sent to electrolyser to

TABLE 4. Optimal combination of components.

Availability	Full	Not full
N_{WG}	5	6
N_{PV}	455	454
P_{el} (kW)	267.801	260.2
M_{tank} (kg)	249.68	230.2
P_{FC} (kW)	361.655	298.1
P_{inv} (kW)	347.6	291
θ_{PV} (deg ree)	51.6	51.2
N_{chr}	19	18

TABLE 5. Optimal costs and reliability indices.

Availability	Full	Not full
J (MUS$/yr)	7.5	7.1
Investment cost (MUS$)	7.5	6.6
ACloss (MUS$/yr)	0	0.6
ELF	0	0.004
LOEE (MWh/yr)	0	8.6
LPSP	0	0.0271
LOLE (h/yr)	0	307.38

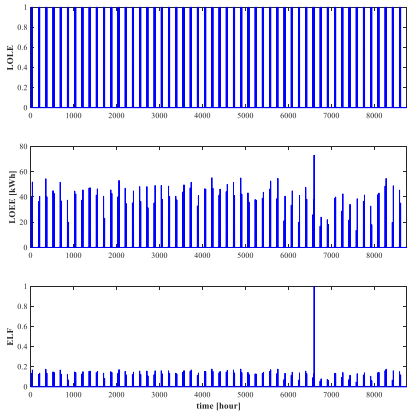

FIGURE 5. Reliability indices (LOLE, LOEE and ELF) over the sample year.

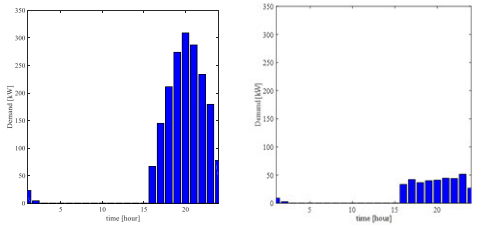

(a) (b)

FIGURE 6. Demand for the sample (a) day 1 and (b) day 2.

produce power when the demand had risen during peak load for both days. The tank stored the energy in itself to support the load when required using electrolyser and FC.

Table 6 gives values for LOEE, LPSP and LOLE for days 1 and 2. Clearly the values for the second day is much lower than the first day as the demand of day 2 is considerably lighter than the first day and thus no load were nearly lost. LOLE and LOEE values for day 1 indicates that the demand was lost for hours 19, 20 and 21 as the demand was larger than the size of inverter installed and therefore, a 5.6 US$/kWh

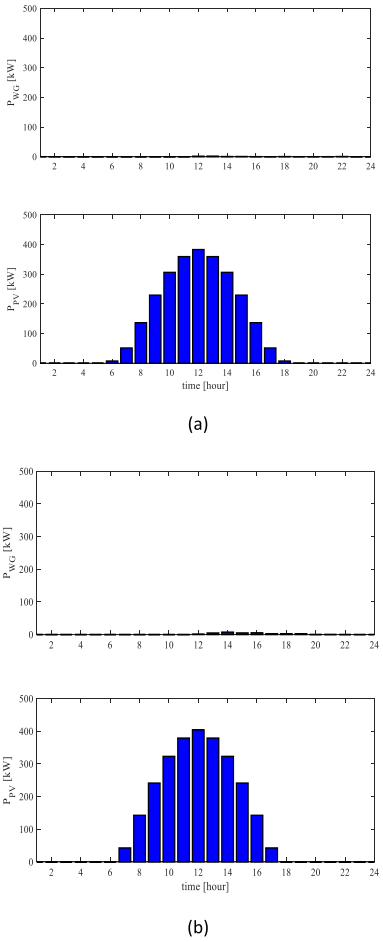

(a)

(b)

FIGURE 7. RES units output for the sample (a) day 1 and (b) day 2.

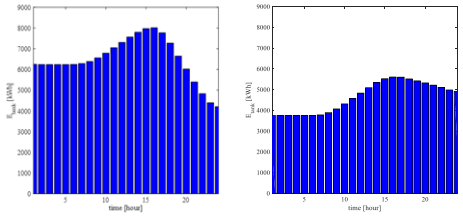

(a) (b)

FIGURE 8. Hourly expected amount of stored energy in the hydrogen tank during the sample (a) day 1 and (b) day 2.

TABLE 6. Reliability indices for the sample days 1&2.

Days	LOEE (kWh/day)	LPSP	LOLE (h/day)
Day 1	98.9	0.055	3
Day 2	0.396	0.0011	0.0132

LOE cost was applied. Note that these numbers cannot be absolute zero as we have a very small percentage of chance for our inverter to fail during a day/year and therefore we will lose our load no matter what the situation is.

VI. CONCLUSION

In our research, we have evidenced from the state-of-the-art literature that on-line charging of EVs using a standalone

HGPS in combination with reliability and economics optimization remains an open challenge. Therefore, our methodology has aimed to address this knowledge gap by designing an optimal multi- vector standalone HGPS to supply a fleet of EVs during a full year with considerations for economic and reliability indices. This paper successfully designed a standalone HGPS, consisting of WT, PV, electrolyser and FC, to supply a load profile of an EV charging station. The data used for simulation represents actual annual solar irradiation and wind speed for the northwest region of Iran. The HGPS is then optimized using PSO to determine the optimal combinations of components with consideration to economics and reliability indices. The optimal combination of components resulted in a high PV/WT ratio due to high capital and maintenance cost for each WT unit. As a result of the optimization, considering unreliable supply from the renewable energy, the investment cost of the HGPS was brought down to 6.6 MUS$ with an ELF of 0.004 (ELF should be less than 0.01) and LPSP of 0.0271. Thus, our proposed multi-vector HGPS modelling offered a reliable and cost-efficient approach to on-line charging of an EV fleet for different days and seasons of a full sample year.

To further explore and demonstrate the different levels of importance for economics and reliability indices, two energy scenarios were considered for standalone HGPS where the first scenario is for winter and high demand and the second scenario is for summer and a lightly loaded day. Despite the difference in the magnitude and timing, the generations are quite similar for PV and WT in the two different scenarios. As for the FC, the stored energy had risen in the tank higher in the first scenario but then depleted faster than the second scenario as it was required to produce more power to meet the higher peak load later in the day. We can conclude from the reliability indices of LOEE, LPSP and LOLE that the EV charging from the peak loading during the winter affected the reliability significantly. In comparison with the EV charging for the lighter loading, the reliability was nearly zero in the analysis for the second day. Thus, we proposed the future works on EV charging HGPS design, which takes into account the uncertainties of wind speed and solar irradiation, to forecast loads on busy days to ensure loads can then be scheduled as it can improve the reliability of the system. To better account for random behaviour of EV drivers, it is recommended to use different assumptions about the daily range, the hours that each EV stays at the site and the percentage of cars stays at the site for the future studies.

REFERENCES

[1] S. Norbu, B. Couraud, V. Robu, M. Andoni, and D. Flynn, "Modeling economic sharing of joint assets in community energy projects under LV network constraints," *IEEE Access*, vol. 9, pp. 112019–112042, 2021, doi: 10.1109/ACCESS.2021.3103480.

[2] P. McCallum, D. P. Jenkins, A. D. Peacock, S. Patidar, M. Andoni, D. Flynn, and V. Robu, "A multi-sectoral approach to modelling community energy demand of the built environment," *Energy Policy*, vol. 132, pp. 865–875, Sep. 2019, doi: 10.1016/j.enpol.2019.06.041.

[3] B. Couraud, P. Kumar, V. Robu, D. Jenkins, S. Norbu, D. Flynn, and A. R. Abhyankar, "Assessment of decentralized reactive power control strategies for low voltage PV inverters," in *Proc. 8th Int. Conf. Power Syst. (ICPS)*, Dec. 2019, pp. 1–6, doi: 10.1109/ICPS48983.2019.9067367.

[4] M. Mokhtar, V. Robu, D. Flynn, C. Higgins, J. Whyte, C. Loughran, and F. Fulton, "Prediction of voltage distribution using deep learning and identified key smart meter locations," *Energy AI*, vol. 6, Dec. 2021, Art. no. 100103, doi: 10.1016/j.egyai.2021.100103.

[5] M. Andoni, V. Robu, B. Couraud, W.-G. Fruh, S. Norbu, and D. Flynn, "Analysis of strategic renewable energy, grid and storage capacity investments via stackelberg-cournot modelling," *IEEE Access*, vol. 9, pp. 37752–37771, 2021, doi: 10.1109/ACCESS.2021.3062981.

[6] S. Norbu, B. Couraud, V. Robu, M. Andoni, and D. Flynn, "Modelling the redistribution of benefits from joint investments in community energy projects," *Appl. Energy*, vol. 287, Apr. 2021, Art. no. 116575, doi: 10.1016/j.apenergy.2021.116575.

[7] B. Couraud, S. Norbu, M. Andoni, V. Robu, H. Gharavi, and D. Flynn, "Optimal residential battery scheduling with asset lifespan consideration," in *Proc. IEEE PES Innov. Smart Grid Technol. Europe*, Oct. 2020, pp. 630–634, doi: 10.1109/ISGT-Europe47291.2020.9248889.

[8] Y. W. Kean, A. Ramasamy, S. Sukumar, and M. Marsadek, "Adaptive controllers for enhancement of stand-alone hybrid system performance," *Int. J. Power Electron. Drive Syst. (IJPEDS)*, vol. 9, no. 3, p. 979, Sep. 2018, doi: 10.11591/ijpeds.v9.i3.pp979-986.

[9] W. Tang, D. Roman, R. Dickie, V. Robu, and D. Flynn, "Prognostics and health management for the optimization of marine hybrid energy systems," *Energies*, vol. 13, no. 18, p. 4676, Sep. 2020, doi: 10.3390/en13184676.

[10] H. Gharavi and M. M. Ardehali, "Imperialist competitive algorithm for optimal design of on-grid hybrid green power system integrated with a static compensator for reactive power management," *J. Renew. Sustain. Energy*, vol. 5, no. 1, Jan. 2013, Art. no. 013115, doi: 10.1063/1.4790816.

[11] A. Khatibzadeh, M. Besmi, A. Mahabadi, and M. R. Haghifam, "Multi-agent-based controller for voltage enhancement in AC/DC hybrid microgrid using energy storages," *Energies*, vol. 10, no. 2, p. 169, Feb. 2017, doi: 10.3390/en10020169.

[12] R. Belfkira, O. Hajji, C. Nichita, and G. Barakat, "Optimal sizing of standalone hybrid wind/PV system with battery storage," in *Proc. Eur. Conf. Power Electron. Appl.*, 2007, pp. 1–10.

[13] L. Xu, X. Ruan, C. Mao, B. Zhang, and Y. Luo, "An improved optimal sizing method for wind-solar-battery hybrid power system," *IEEE Trans. Sustain. Energy*, vol. 4, no. 3, pp. 774–785, Jul. 2013, doi: 10.1109/TSTE.2012.2228509.

[14] M. Hatti, A. Meharrar, and M. Tioursi, "Power management strategy in the alternative energy photovoltaic/PEM fuel cell hybrid system," *Renew. Sustain. Energy Rev.*, vol. 15, no. 9, pp. 5104–5110, Dec. 2011, doi: 10.1016/j.rser.2011.07.046.

[15] M. Z. Vahid, M. Hajivand, M. Moshkelgosha, N. Parsa, and H. Mansoori, "Optimal, reliable and economic designing of renewable energy photovoltaic/wind system considering different storage technology using intelligent improved salp swarm optimisation algorithm, commercial application for Iran country," *Int. J. Sustain. Energy*, vol. 39, no. 5, pp. 465–485, May 2020, doi: 10.1080/14786451.2020.1716758.

[16] S. M. Lawan and W. A. W. Z. Abidin, "A review of hybrid renewable energy systems based on wind and solar energy: Modeling, design and optimization," in *Wind Solar Hybrid Renewable Energy System*. IntechOpen, 2020, doi: 10.5772/intechopen.85838.

[17] J. Kartite and M. Cherkaoui, "Optimal sizing of hybrid renewable PV/Wind battery system using LPSP methods," in *Proc. 6th Int. Conf. Syst. Control (ICSC)*, May 2017, pp. 226–230, doi: 10.1109/ICoSC.2017.7958737.

[18] I. Sansa, R. Villafafila, and N. M. Bellaaj, "Optimal sizing design of an isolated microgrid using loss of power supply probability," in *Proc. IREC 6th Int. Renew. Energy Congr.*, Mar. 2015, pp. 1–7, doi: 10.1109/IREC.2015.7110941.

[19] H. X. Yang, W. Zhou, L. Lu, and Z. Fang, "Optimal sizing method for stand-alone hybrid solar-wind system with LPSP technology by using genetic algorithm," *Sol. Energy.*, vol. 82, no. 4, pp. 354–367, 2008, doi: 10.1016/j.solener.2007.08.005.

[20] B. O. Bilal, V. Sambou, P. A. Ndiaye, C. M. F. Kébé, and M. Ndongo, "Optimal design of a hybrid solar-wind-battery system using the minimization of the annualized cost system and the minimization of the loss of power supply probability (LPSP)," *Renew. Energy*, vol. 35, no. 10, pp. 2388–2390, 2010, doi: 10.1016/j.renene.2010.03.004.

[21] E. Koutroulis, D. Kolokotsa, A. Potirakis, and K. Kalaitzakis, "Methodology for optimal sizing of stand-alone photovoltaic/wind-generator systems using genetic algorithms," *Sol. Energy*, vol. 80, no. 9, pp. 1072–1088, Sep. 2006, doi: 10.1016/j.solener.2005.11.002.

[22] T. Senjyu, D. Hayashi, N. Urasaki, and T. Funabashi, "Optimum configuration for renewable generating systems in residence using genetic algorithm," *IEEE Trans. Energy Convers.*, vol. 21, no. 2, pp. 459–466, Jun. 2006, doi: 10.1109/TEC.2006.874250.
[23] G. L. Terra, G. Salvina, and T. G. Marco, "Optimal sizing procedure for hybrid solar wind power systems by fuzzy logic," in *Proc. IEEE Medit. Electrotech. Conf.*, May 2006, pp. 865–868.
[24] O. Ekren and B. Y. Ekren, "Size optimization of a PV/wind hybrid energy conversion system with battery storage using simulated annealing," *Appl. Energy*, vol. 87, no. 2, pp. 592–598, 2010, doi: 10.1016/j.apenergy.2009.05.022.
[25] M. Pirhaghshenasvali and B. Asaei, "Optimal modeling and sizing of a practical hybrid wind/PV/diesel generation system," in *Proc. 5th Annu. Int. Power Electron., Drive Syst. Technol. Conf.*, Feb. 2014, pp. 506–511, doi: 10.1109/PEDSTC.2014.6799427.
[26] M. Bashir and J. Sadeh, "Optimal sizing of hybrid wind/photovoltaic/battery considering the uncertainty of wind and photovoltaic power using Monte Carlo," in *Proc. 11th Int. Conf. Environ. Elect. Eng.*, May 2012, pp. 1081–1086, doi: 10.1109/EEEIC.2012.6221541.
[27] A. K. Kaviani, G. H. Riahy, and S. M. Kouhsari, "Optimal design of a reliable hydrogen-based stand-alone wind/PV generating system, considering component outages," *Renew. Energy*, vol. 34, no. 11, pp. 2380–2390, Nov. 2009, doi: 10.1016/j.renene.2009.03.020.
[28] A. M. Andwari, A. Pesiridis, S. Rajoo, R. Martinez-Botas, and V. Esfahanian, "A review of battery electric vehicle technology and readiness levels," *Renew. Sustain. Energy Rev.*, vol. 78, pp. 414–430, Oct. 2017, doi: 10.1016/j.rser.2017.03.138.
[29] A. Gaurav and A. Gaur, "Modelling of hybrid electric vehicle charger and study the simulation results," in *Proc. Int. Conf. Emerg. Frontiers Elect. Electronic Technol. (ICEFEET)*, Jul. 2020, pp. 1–6, doi: 10.1109/ICEFEET49149.2020.9187007.
[30] A. Unni, A. S. Kumar, R. Manoj, S. Sunil, and J. S. Vc, "Design and simulation of test-bed for of emulation electric vehicle dynamics," in *Proc. 16th Int. Conf. Ecol. Vehicles Renew. Energies*, Jun. 2021, pp. 1–6, doi: 10.1109/ever52347.2021.9456618.
[31] C. Yang, J. Tang, and Q. Shen, "Impact of electric vehicle battery parameters on the large-scale electric vehicle charging loads in power distribution network," in *Proc. 16th Int. Conf. Control, Autom., Robot. Vis. (ICARCV)*, Dec. 2020, pp. 56–60, doi: 10.1109/ICARCV50220.2020.9305326.
[32] K. Chaudhari, A. Ukil, K. N. Kumar, U. Manandhar, and S. K. Kollimalla, "Hybrid optimization for economic deployment of ESS in PV-integrated EV charging stations," *IEEE Trans. Ind. Informat.*, vol. 14, no. 1, pp. 106–116, Jan. 2018, doi: 10.1109/TII.2017.2713481.
[33] S. W. Hadley and A. A. Tsvetkova, "Potential impacts of plug-in hybrid electric vehicles on regional power generation," *Electr. J.*, vol. 22, no. 10, pp. 56–68, Dec. 2009, doi: 10.1016/j.tej.2009.10.011.
[34] D. Said, S. Cherkaoui, and L. Khoukhi, "Scheduling protocol with load managementfor EV charging," in *Proc. IEEE Global Commun. Conf.*, Dec. 2014, pp. 362–367, doi: 10.1109/GLOCOM.2014.7036835.
[35] Q. Huang, Q.-S. Jia, L. Xia, X. Guan, and X. Xie, "EV charging load scheduling following uncertain renewable energy supply by stochastic matching," in *Proc. IEEE Int. Conf. Automat. Sci. Eng.*, Aug. 2014, pp. 137–142, doi: 10.1109/CoASE.2014.6899317.
[36] C. Liu, K. T. Chau, D. Wu, and S. Gao, "Opportunities and challenges of vehicle-to-home, vehicle-to-vehicle, and vehicle-to-grid technologies," *Proc. IEEE*, vol. 101, no. 11, pp. 2409–2427, Nov. 2013, doi: 10.1109/JPROC.2013.2271951.
[37] D. Lu, B. Wang, Y. Wang, H. Zhou, Q. Liang, Y. Peng, and T. Roskilly, "Optimal operation of cascade hydropower stations using hydrogen as storage medium," *Appl. Energy*, vol. 137, pp. 56–63, Jan. 2015, doi: 10.1016/j.apenergy.2014.09.092.
[38] A. P. Roskilly, P. C. Taylor, and J. Yan, "Energy storage systems for a low carbon future—In need of an integrated approach," *Appl. Energy*, vol. 137, pp. 463–466, Jan. 2015, doi: 10.1016/j.apenergy.2014.11.025.
[39] A. Ajanovic and R. Haas, "Prospects and impediments for hydrogen and fuel cell vehicles in the transport sector," *Int. J. Hydrogen Energy*, vol. 46, no. 16, pp. 10049–10058, Mar. 2021, doi: 10.1016/j.ijhydene.2020.03.122.
[40] G. Bristowe and A. Smallbone, "The key techno-economic and manufacturing drivers for reducing the cost of power-to-gas and a hydrogen-enabled energy system," *Hydrogen*, vol. 2, no. 3, pp. 273–300, Jul. 2021, doi: 10.3390/hydrogen2030015.
[41] A. Saeedmanesh, M. A. M. Kinnon, and J. Brouwer, "Hydrogen is essential for sustainability," *Current Opinion Electrochemistry*, vol. 12, pp. 166–181, Dec. 2018, doi: 10.1016/j.coelec.2018.11.009.
[42] C. W. Babbitt, "Sustainability perspectives on lithium-ion batteries," *Clean Technol. Environ. Policy*, vol. 22, no. 6, pp. 1213–1214, Aug. 2020, doi: 10.1007/s10098-020-01890-3.
[43] K. Strunz and E. Kristinabrock, "Stochastic energy source access management: Infrastructure-integrative modular plant for sustainable hydrogen-electric co-generation," *Int. J. Hydrogen Energy*, vol. 31, no. 9, pp. 1129–1141, Aug. 2006, doi: 10.1016/j.ijhydene.2005.10.006.
[44] M. Jahannoosh, S. A. Nowdeh, A. Naderipour, H. Kamyab, I. F. Davoudkhani, and J. J. Klemes, "New hybrid meta-heuristic algorithm for reliable and cost-effective designing of photovoltaic/wind/fuel cell energy system considering load interruption probability," *J. Cleaner Prod.*, vol. 278, Jan. 2021, Art. no. 123406, doi: 10.1016/j.jclepro.2020.123406.
[45] N. W. Technologies. (Nov. 2015). *Costs Associated With Non-Residential Electric Vehicle Supply Equipment Factors to Consider in the Implementation of Electric Vehicle Charging Stations*. Accessed: Jan. 6, 2021. [Online]. Available: https://afdc.energy.gov/files/u/publication/evse_cost_report_2015.pdf
[46] *EV Charger Availability*. Accessed: Jan. 6, 2021. [Online]. Available: https://www.greencarreports.com/news/1076151_reliability-of-electric-car-charging-networks-varies-wildly-study-says
[47] H. A. Gabbar, M. R. Abdussami, and I. M. Adham, "Optimal planning of nuclear-renewable micro-hybrid energy system by particle swarm optimization," *IEEE Access*, vol. 8, pp. 181049–181073, 2020, doi: 10.1109/ACCESS.2020.3027524.
[48] M. A. Gennert and A. L. Yuille, "Determining the optimal weights in multiple objective function optimization," in *Proc. 2nd Int. Conf. Comput. Vis.*, 1988, pp. 5–8, doi: 10.1109/CCV.1988.589974.
[49] A. Ratnaweera, S. K. Halgamuge, and H. C. Watson, "Self-organizing hierarchical particle swarm optimizer with time-varying acceleration coefficients," *IEEE Trans. Evol. Comput.*, vol. 8, no. 3, pp. 240–255, Jun. 2004.

HANI GHARAVI AHANGAR (Member, IEEE) was born in Babol, Iran. He received the Ph.D. degree in electrical engineering from Queen's University Belfast, U.K., in 2020.

He is currently a Senior Power System Engineer with Elgin Energy, Dublin, Ireland, that is a Solar Development/Installation company in Ireland, U.K., Germany and Australia. He is shaping Ireland's electricity future targeting an ambitious 95% pure renewable generation nationwide by 2030. His research interests include HV/LV power system analysis, renewable energy, optimization, artificial intelligence, and .smart grids.

WENG KEAN YEW (Member, IEEE) was born in Selangor, Malaysia. He received the Ph.D. degree in electrical engineering from the National Energy University, Malaysia, in 2019.

He is currently an Assistant Professor with Heriot-Watt University Malaysia, Putrajaya, Malaysia. His research interests include hybrid green power systems, renewable energy, artificial intelligence, and smart grids.

DAVID FLYNN (Member, IEEE) received the B.Eng. degree (Hons.) in electrical and electronic engineering, the M.Sc. degree (Hons.) in microsystems, and the Ph.D. degree in microscale magnetic components from Heriot-Watt University, Edinburgh, in 2002, 2003, and 2007, respectively. He is currently a Professor in smart systems engineering at the University of Glasgow. He is also the Founder of the Smart Systems Group (SSG), Heriot-Watt University, and the Associate Director of the U.K.'s National Centre for Energy Systems Integration. He has expertise in systems engineering and cyber-physical systems (CPS). His research interests include challenges, opportunities, and underpinning technologies within cyber-physical systems as to promote sustainability and create resilience in systems, organizations, networks, and societies.